JOURNAL OF MATERIALS SCIENCE 27 (1992) 1748–1756

Formation of dense and non-agglomerated lead oxide particles by spray pyrolysis

F. KIRKBIR, D. KATZ*, R. LYSSE, J. D. MACKENZIE
Department of Material Science and Engineering, University of California, Los Angeles, CA 90024, USA

Submicrometre, highly pure and dense PbO particles were synthesized by pyrolysis of a spray of a lead nitrate, $Pb(NO_3)_2$ solution generated by an ultrasonic transducer in a tubular-flow reactor at 300–800 °C and at various carrier gas flow rates. The produced particles were non-agglomerated, non-porous, and mainly tetragonal PbO above 500 °C. Below this temperature, the conversion could not be completed. The high purity, completely densified particles could be obtained at high gas flow rates. The observed particle yields higher than 90%, indicated the high efficiency of this process. Preheating of the mist before the pyrolysis stage was found to be necessary for densification of the particles. Experiments indicated that the spray was dried at the end of the preheating stage forming dense and non-porous $Pb(NO_3)_2$ particles. These non-porous particles decomposed and shrunk to PbO particles without any particle bursting into pieces. Therefore, it was concluded that the decomposition occurred through the liquid phase allowing the evolution of gaseous reaction products by bubbling.

1. Introduction

The spray pyrolysis technique has been employed to produce a variety of simple (MgO, NiO, ZrO_2, ZnO) and mixed (Y_2O_3–ZrO_2, ZrO_2–SiO_2) metal oxide powders from solutions of metal alkoxides or metal salts in a continuous manner [1–7]. In this technique, the liquid droplets generated from a solution by an atomizer and carried away by an inert gas are dried and decomposed to an oxide powder by passing through several heaters kept at different temperatures.

The spray of the solution can be generated by various atomizers (compressed air nebulizer, ultrasonic nebulizer, spinning disc, etc.) with which liquid particles up to 100 μm in diameter can be obtained [8]. In the present investigation, an ultrasonic generation technique was preferred due to its major advantage of producing much finer (< 10 μm), and therefore faster drying, particles than the other techniques. Furthermore, the particle size and the particle concentration can independently be controlled with this technique.

The solid particle is produced from the liquid droplet by simultaneous or consecutive drying and thermal decomposition steps. A major disadvantage of this process is the formation of a crust at the drying step by precipitation of solute close to the surface of the droplet due to rapid evaporation of solution, resulting into hollow particles [9]. This prevents the evolution of the solvent trapped inside the particle and eventually either a low density particle is obtained or, if the developing inner pressure is sufficient, the particle explosion is observed leaving hollow shell fragments behind [2, 6, 7]. Also, as a result of the crust formation, the trapped solute or solvent can decrease the purity of the particle, consequently degrading the quality of the ceramic produced for electronical and optical applications. Then, it is necessary to treat further these powders by heating and/or grinding to obtain high purity densified ceramic bodies at the sintering stage. This treatment will increase the processing time of fine ceramics. In conclusion, generation of highly dense and highly pure as well as nonagglomerated particles within the aerosol reactor becomes an important factor for the successful applications of the spray pyrolysis process.

Dubois *et al.* [1] used a furnace which had a thermal gradient for densification of the particles. They have found that as-prepared particles were amorphous and contained impurities. When the additional furnace, operated at a higher temperature was used, the particles were broken. They concluded that a heat treatment of the as-prepared powder at low temperatures is required for the particle crystallization and purification. Ishizawa *et al.* [3] have proposed that the densified particles can be produced by the use of metal alkoxides. They argued that during the pyrolysis, a three-dimensional polymer network was formed due to polymerization reactions of metal alkoxides which is preventing the formation of the crust and allowing evolution of gaseous products from the particle without its rupture. On the other hand, Zhang *et al.* [7] intended to obtain dense particles using metal salts by investigating the solution parameters and physical characteristics of the precursor. They concluded that

* *Present address*: Plasma Materials Inc., 222 W. Orange Grove Ave, Burbank, CA 91502, USA.

0022–2461

the densified powders can be obtained when the initial relative solution saturation is 10^{-2} and the precipitated salt is permeable to the diffusing and evaporating solvent remaining inside the particle.

In the present investigation, we explored the spray pyrolysis process to determine the experimental conditions, such as solution concentration, the gas flow rate (i.e. the residence time in the pyrolysis chamber) and the pyrolysis temperature to obtain highly dense and pure particles, and to have an insight into the particle formation mechanism. We produced submicrometer PbO particles from lead nitrate solutions. PbO was chosen because of its high infrared cutoff (17 μm) and high melting point (886 °C) which makes this material a candidate for transmitting infrared. Moreover there is a scarce amount of knowledge on the production of PbO particles.

2. Experimental procedure

Fine PbO particles were prepared by spray pyrolysis of a $Pb(NO_3)_2$ solution in a vertical quartz tubular-flow reactor (ID:2.2 cm) at atmospheric pressure. A schematic diagram of the experimental system is given in Fig. 1.

$Pb(NO_3)_2$ was dissolved in water. The solution concentrations were 3.24×10^{-2} and 4×10^{-3} mol l^{-1}. The mist was prepared from these solutions by employing an ultrasonic transducer which can be operated at 1.7 MHz frequency. The amount of the mist generated was determined by measuring the weight decrease of the solution fed to the pyrex mist chamber. The mist was carried away from the chamber by a flow of He gas. The experiments were performed at two different gas flow rates, 1500 and 3000 cc min^{-1}. The amounts of the mist generated at these flow rates were approximately 25 and 47 g h^{-1}, respectively.

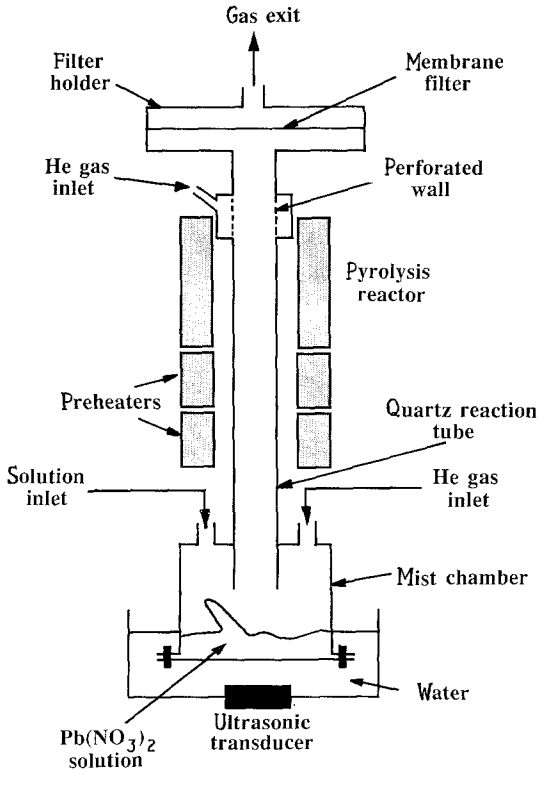

Figure 1 Schematic diagram of the experimental system.

The mist carried with He gas was preheated before entering into the high temperature pyrolysis section. The purpose of this preheating was to aid the densification of the powder. The preheating section consisted of two heating zones which were 25 cm long and heated at 60 and 150 °C. The mist was pyrolyzed in the reaction tube heated by a 60 cm long gold-image furnace at temperatures between 300–800 °C. The reported temperatures were those measured by thermocouples of the temperature controllers, which were placed on the inner surface of the heaters at the middle of each heating zone. The gas residence times were 1.42 and 1.12 s at the preheating sections and 1.98 to 1.16 s at the pyrolysis section at 1500 cc min^{-1} gas flow rate.

There exists a radial temperature gradient at the reactor exit which can be responsible for the deposition of the particles on the surface of the tube due to the thermophoretic force. The amount of this deposition can be as high as 40% of the particles at high temperatures [10]. To prevent thermophoretic deposition, a cold helium gas was radially flown from the perforated surface of the reaction tube at a rate of 1000 cc min^{-1}.

The solid particles were collected from the gas stream by a teflon membrane filter which had 0.2 μm pores. The steel filter holder was heated at 125 °C to prevent the condensation of the water vapour on the particles to obtain a dry filter cake. The yield was calculated by comparing the amount of the particles collected on the filter with the amount of $Pb(NO_3)_2$ fed to the reactor according to the following stoichiometry of the reaction:

$$Pb(NO_3)_2 \rightarrow PbO + 2NO_2 + 1/2\,O_2 \quad (1)$$

The particle diameters were measured from the micrographs of the particles collected on the membrane filter, using a transmission electron microscope (TEM). The specific surface area of the particles was determined by a single-point Braunauer–Emmer–Teller (BET) method at the boiling temperature of N_2. The crystalline structure of the particles was determined by an X-ray diffraction (XRD) method. Differential thermal analysis (DTA) and thermal gravimetric analysis (TGA) were done under an inert atmosphere using He flow (heating rate was 10 °C min^{-1}). The density of the powder sample was determined by a pycnometer using helium gas. The nitrogen content of the samples was determined by combustion of a sample at 950 °C and measurement of the N_2 concentration in the gas by thermal conductivity.

3. Results

Table I gives the details of the experimental results as a function of gas flow rate and temperature. In general, the particle yields were very high up to 700 °C. Then it decreased to a very low value at 800 °C indicating that important amounts of PbO could not be recovered as particles on the filter at this temperature. However, at the high gas flow rate experiments, it was

TABLE I Effects of experimental conditions on particle properties

Gas flow rate (cc min^{-1})	Pyrolysis temperature (°C)	Yield (%)	Density (g cm^{-3})	BET area (m^2 g^{-1})	Equivalent size (μm)	Crystalline structure
1500	300	97	4.27	1.5	0.93	$Pb(NO_3)_2$
1500	400	91	–	3.1	–	$Pb(NO_3)_2/Pb(OH)_2$/?
1500	450	97	5.24	3.1	0.37	?
1500	500	100	7.85	3.1	0.25	Red PbO
1500	600	94	8.94	2.0	0.33	Red PbO
1500	700	88	9.01	1.6	0.42	Red/yellow PbO
1500	750	64	–	–	–	Red/yellow PbO
1500	800	20	–	–	–	Red/yellow/? PbO
3000	500	93	7.24	2.6	0.32	Red $PbO/Pb(OH)_2$
3000	600	92	9.40	1.2	0.56	Red/yellow PbO
3000	700	94	9.51	1.7	0.37	Red PbO
3000	750	90	9.85	1.4	0.43	Red PbO
3000	800	53	–	–	–	Red/yellow PbO

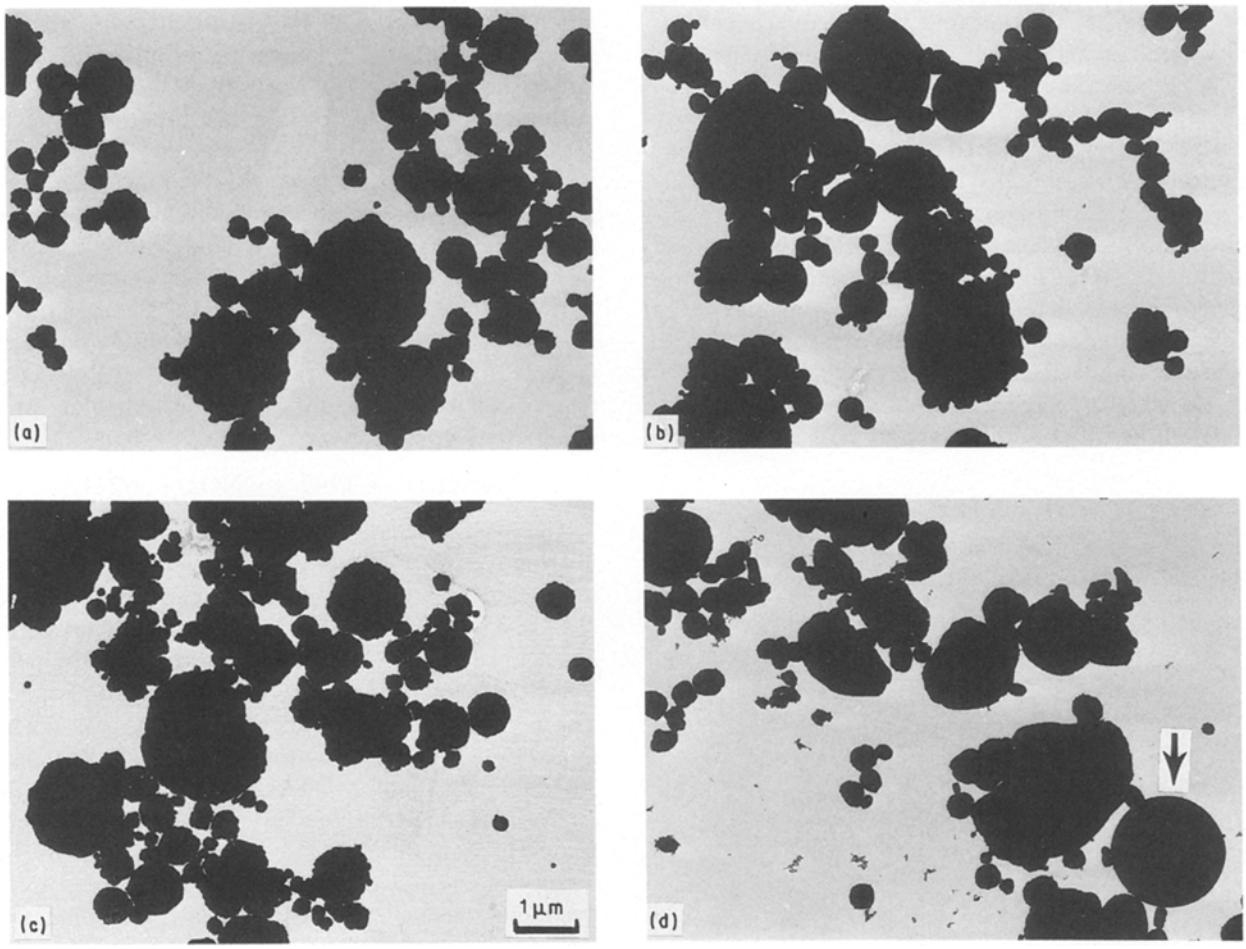

Figure 2 TEM micrographs of the PbO particles synthesized at 3000 cc min^{-1} flow rate with a solution concentration of 3.24×10^{-2} mol l^{-1} at temperature (a) 500 °C, (b) 600 °C, (c) 700 °C, (d) 750 °C.

possible to obtain high yields at temperatures as high as 750 °C.

TEM micrographs given in Fig. 2 have shown that the particles were non-agglomerated. The particle size was not appreciably affected from the gas flow rate and the pyrolysis temperature. The mean particle size was around 0.53 μm and the geometric standard deviation, σ_p was 1.71 (approximately 350 particles were counted). Although the particles were spherical in shape, mostly, they have rough surfaces. The small amount produced at high temperatures were perfectly spherical in shape, as indicated, by an arrow in Fig. 2 for 750 °C.

The DTA and TGA of the starting material $Pb(NO_3)_2$ given in Fig. 3 shows that the pyrolysis proceeded in stages. The endothermic peaks appeared

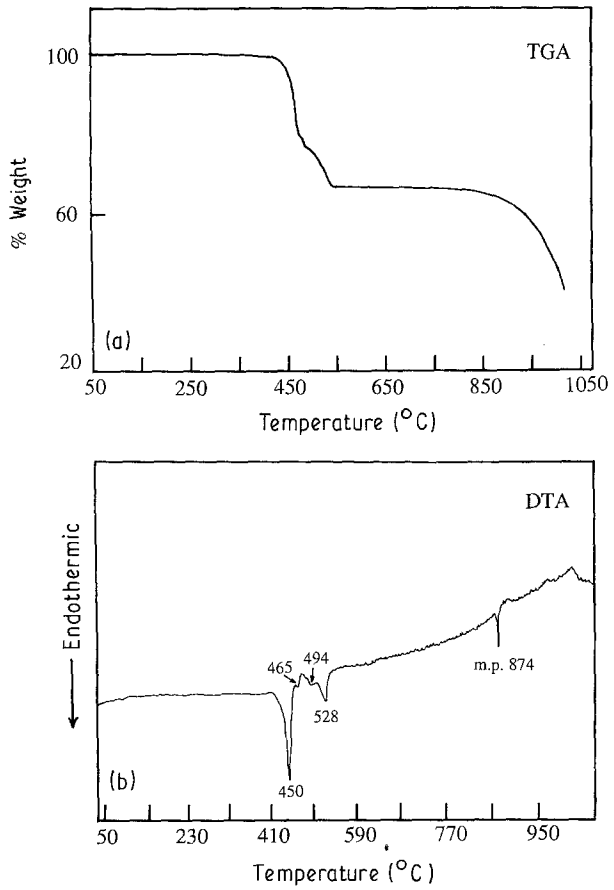

Figure 3 Thermal analysis of the precursor, $Pb(NO_3)_2$ using (a) TGA and (b) DTA.

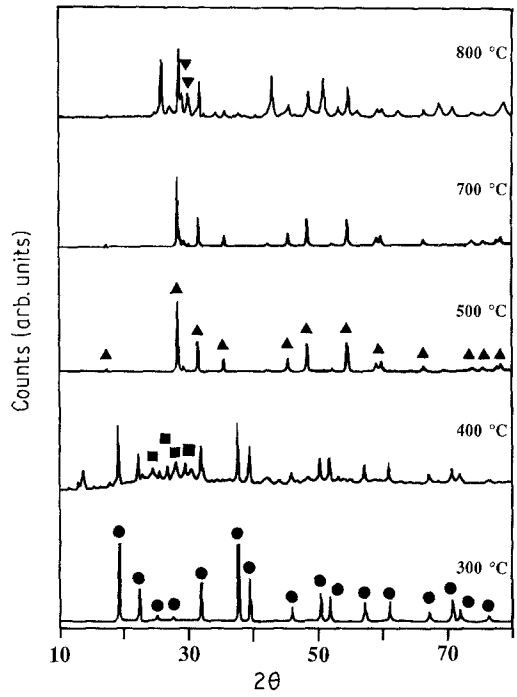

Figure 4 XRD patterns of the PbO particles synthesized at various pyrolysis temperatures, a 1500 cc min^{-1} flow rate and with a solution concentration of 3.24×10^{-2} mol l^{-1}. ● $Pb(NO_3)_2$, ■ $Pb(NO_3)_2 \cdot Pb(OH)_2$, ▲ Red PbO, ▼ Yellow PbO.

in DTA between 412 and 538 °C coupled with the weight decreases in TGA were related with the thermal decomposition of $Pb(NO_3)_2$. The 33.7% weight decrease, which occurred up to 538 °C, corresponded to total denitration of initial content, as determined from the stoichiometry of the reaction. From the thermal analysis results, the decomposition reaction can be divided into four consecutive stages. These stages occurred between 412–464, 464–478, 478–511 and 511–538 °C corresponding to 21.1%, 3.3%, 2.2% and 7.2% weight decreases of the initial content, respectively. The last endothermic peak that appeared around 874 °C was attributed to the melting of PbO. The reported melting point is 886 °C [11]. The weight decrease which became appreciable after 840 °C was because of the evaporation of PbO.

The progression of the reaction within the particles as a function of the pyrolysis temperature can be followed by XRD patterns of the particles given in Fig. 4. At 300 °C, the particles were crystalline $Pb(NO_3)_2$. Above 500 °C, the conversion of $Pb(NO_3)_2$ to PbO reached completion. All of the diffraction peaks that appeared could not exactly be identified from the known patterns of lead oxide nitrates for the particles synthesized at temperatures between 300 and 500 °C. However, the diffraction lines due to $Pb(NO_3)_2$, $Pb(OH)_2$ and PbO were determined. Furthermore, the high weight losses observed by TGA indicated that the conversion was not complete at these temperatures and the particles contained nitrates or nitrites of lead.

Crystalline lead oxide exists in two forms: litharge which is red and tetragonal and massicot which is yellow and orthorhombic. Although all of the synthesized powders were in different shades of yellow and tetragonal to the orthorhombic phase, change occurs around 489 °C [12], forming mainly tetragonal PbO (> 95%) at temperatures above 500 °C. However, at 800 °C, an unidentified phase of lead oxide was obtained together with tetragonal and orthorhombic phase for the particles synthesized at 1500 cc min^{-1}.

Infrared spectra of the particles at the low flow rate are shown in Fig. 5 as a function of temperature. The uppermost spectrum corresponds to that of commercial $Pb(NO_3)_2$ and agrees with that reported in the literature [13]. The absorption bands appearing at 1763, 1380–1315, 832, 805 and 722 cm^{-1} are due to the vibrations of nitrate ion NO_3^{-1} [14]. The intensity of these bands decreased with increasing temperature from 300–500 °C because of the removal of nitrates from the particles which was also followed by XRD. However, although the complete conversion was expected at 500 °C, the absorption band consistently remaining around 1380 cm^{-1}, suggesting the presence of nitrates or nitrites in the particles synthesized above 500 °C.

The new bands appeared around 1440, 855, 840, 690 cm^{-1} in the spectra of the products, synthesized above 500 °C. The bands at 855 and 840 cm^{-1} were either due to lead nitrite or lead oxide nitrates [14, 15]. The bands at 1440 and 690 cm^{-1} were similar to those observed by Margulis *et al.* [14] which were explained by the presence of lead oxide nitrates. Chemical analysis for nitrogen showed that the amount of the nitrates and/or nitrites were between 2–3% for particles synthesized at 500 °C. The weight

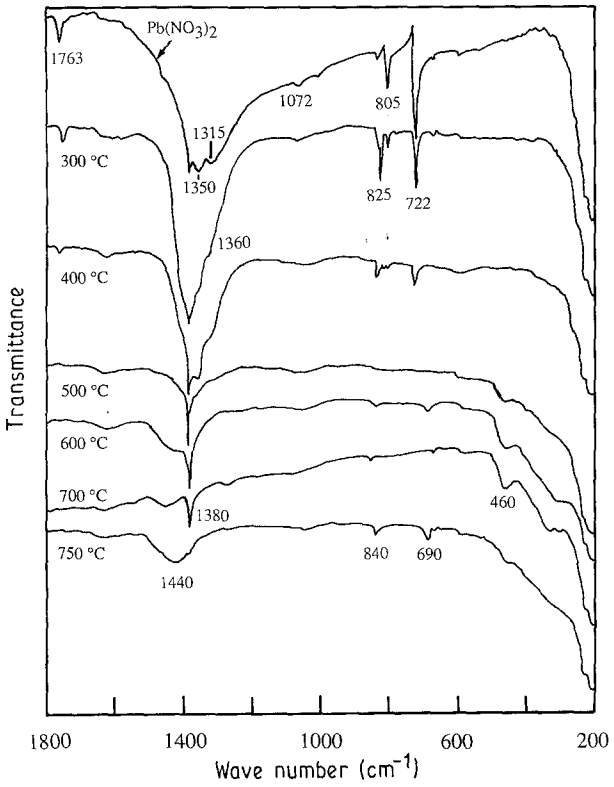

Figure 5 Infrared spectrum of the PbO particles synthesized at 1500 cc min^{-1} flow rate and with a solution concentration of 3.24×10^{-2} mol l^{-1}.

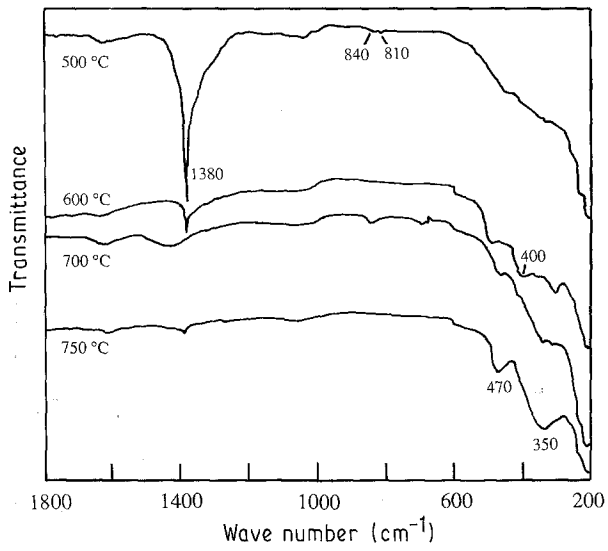

Figure 6 Infrared spectrum of the PbO particles synthesized at 3000 cc min^{-1} flow rate with a solution concentration of 3.24×10^{-2} mol l^{-1}.

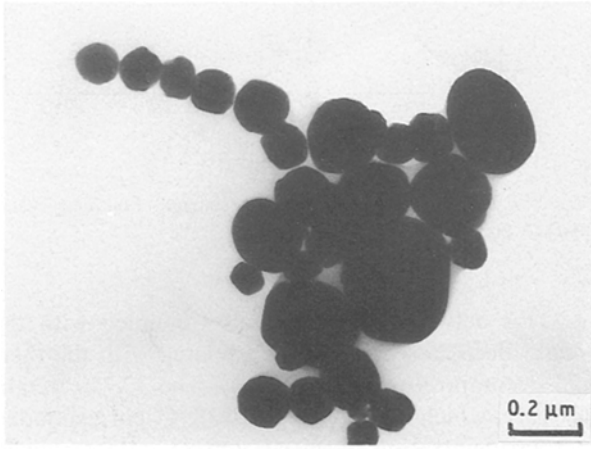

Figure 7 TEM micrographs of the PbO particles synthesized at a solution concentration of 4×10^{-3} mol l^{-1}, a synthesis temperature of 500 °C and a flow rate of 1500 cc min^{-1}.

decrease determined by TGA also implied that their presence was not expected to be higher than 2–3%.

Increasing flow rate, that is decreasing residence time in the reactor, affected both the crystallinity (Table I) and the purity of the particles (Fig. 6). The particles which were synthesized at 500 °C contained appreciable amounts of unconverted $Pb(NO_3)_2$ as can easily be seen from XRD pattern and i.r. spectrum. Occurrence of both forms of crystalline PbO, i.e. tetragonal and orthorhombic was observed at 600 °C. Above 600 °C, particles were mainly high purity tetragonal PbO without any indication of infrared absorption due to nitrates or nitrites.

The particles were highly dense (Table I). The bulk density of $Pb(NO_3)_2$ is 4.53 g cm^{-3} [11]. The bulk densities of tetragonal and orthorhombic PbO are 9.53 and 8.0 g cm^{-3}, respectively [11]. The $Pb(NO_3)_2$ particles synthesized at 300 °C were 94% dense. The density of the particles increased both with increasing temperature and increasing gas flow rate. The particles prepared at the low flow rate and at 500–700 °C were 82–95% dense. At the high flow rate, the particles were completely densified. However, the density of the particles synthesized at 750 °C and 3000 cc min^{-1} was higher than expected, at 9.85 g cc^{-1}. The bulk density of Pb is 11.34 g cc^{-1} [11]. This high density was possibly due to the reduction of PbO to Pb with increasing temperature. It should also be noted that the smooth preheating of the gas was found to be essential to obtain fully densified particles. For example, the particles synthesized at 700 °C and 3000 cc min^{-1} without preheating were not dense at 7.97 g cc^{-1}, whereas at the same conditions but with preheating, fully dense, 9.51 g cc^{-1} particles were obtained.

Moreover, the equivalent size of the particles estimated by using BET surface area and the measured density was close to the size determined by TEM indicating that the particles were not only dense, but also did not contain any porosity. However, the equivalent sizes, ranged between 0.25–0.56 µm were generally smaller than the TEM size, of 0.53 µm, because of the rough particle surface.

Preliminary experiments were done to decrease the particle size by decreasing the concentration of salt solution. The particles shown in Fig. 7, synthesized at 4×10^{3} mol l^{-1}, were 0.27 µm. TEM micrographs indicated that they have smoother surfaces than the particles synthesized at a higher concentration, 3.24×10^{-2} mol l^{-1}.

4. Discussions

In this investigation, fine PbO particles were synthesized by the spray pyrolysis of $Pb(NO_3)_2$ solution.

The spray was generated by an ultrasonic transducer, then dried in the preheating zone and finally pyrolyzed. Each of these processes can be understood and the solid PbO particle formation from the liquid particle can be explained by simple quantitative models. Calculations given below were done for a 1500 cc min^{-1} gas flow rate.

When the salt solution is excited by high frequency ultrasonic vibrations, a fountain above the solution is formed. The ultrasonic vibrations generate capillary waves on the fountain surface and particles form by the rupture of the wave crests. Kelvin's equation which predicts the wavelength of these capillary waves is related to the particle size with an experimental correction factor [16]

$$d_p = 0.34(8\pi\sigma^*/\rho f^2)^{1/3} \quad (2)$$

where d_p is the mean particle size (cm), σ^* is the surface energy of the solution (erg cm^{-2}), ρ is the density of the solution (g cm^{-3}) and f is the frequency of the ultrasonic transducer (Hz). The estimated mist particle size was 2.92 μm (the water properties were used in the calculations since the solution was very dilute). If this mist particle was completely converted and densified to PbO, the final size of the particles collected on the filter would be 0.27 μm. However, the experimentally obtained size was 0.53 μm, suggesting that the initial mist particles were bigger than the one estimated by Equation 2.

The sprays of various salt or alkoxide solutions were generated at the same frequency used in the present experiments (1.7 MHz) by other researchers to synthesize metal oxide fine particles [3–5]. They have also found that the experimental size was approximately two times bigger than the theoretical one. They have prepared 0.24 μm Y_2O_3 stabilized ZrO_2 [3], 1 μm ZrO_2–SiO_2 [4] and 0.15 μm ZnO [5] particles whereas the theoretical sizes were 0.12 μm, 0.49 μm and 0.086 μm, respectively. They have argued that the closed pores within the particles were responsible for the discrepancy between the theoretical and the experimental sizes. This seems to be a reasonable explanation as it is usual to obtain low density particles by spray pyrolysis due to fast drying and chemical reaction rates, which cause rapidly developing solid structures at the particle surface to be impermeable to the solvent or reaction products. As a result of this process, closed pores can be formed inside the particle. However, we obtained high density particles. Therefore, there must be another reason for the synthesis of particles bigger than expected.

The mist particles form in the vicinity of the fountain where the gas phase particle concentration is the highest. If the generated particles cannot be rapidly carried away from the fountain and not quickly diluted, the liquid particles can easily grow by coagulation because of the ultrasonic waves and Brownian motion. Indeed, it has been found that the increase in the gas flow rate from 1 l min^{-1} to 10 l min^{-1} decreased the size of the particles generated by ultrasonic vibrations from 10 μm to 3 μm [8]. Therefore, it was presumed that the coagulation in the mist chamber was responsible for the unexpected bigger size of the mist particle. The coagulation in the reaction tube was negligible as estimated by Smoluchowski's model [17].

The appreciable decomposition of $Pb(NO_3)_2$ occurs above 250 °C [18]. Therefore, no chemical reaction is expected in the preheating section of the reaction tube kept below 150 °C. In this section, the water started to evaporate, the mist particle shrunk and finally dried. The SEM picture (Fig. 8) shows the dried $Pb(NO_3)_2$ particles when the pyrolysis section was operated at 150 °C. The particles were fully spherical with smooth surfaces, non-porous and 94% dense. A small amount of these particles had big holes, as indicated in Fig. 8 by an arrow, due to the particle implosion which is a common feature of spray drying [19]. The average particle size was 0.83 μm ($\sigma_p = 1.57$) corresponding to the initial mist size of 6.23 μm. For the constant drying rate of the liquid droplet, the following equation can be written [19]:

$$\frac{dw}{dt} = \frac{2\pi k d_{av}(T_a - T_s)}{\lambda} \quad (3)$$

Here dw/dt is the drying rate (g s^{-1}), k is the thermal conductivity of helium (cal cm^{-1} s^{-1} K^{-1}), d_{av} is the average of the particle sizes at the entrance and at the exit of the drying section (cm), λ is the latent heat of vaporization (cal g^{-1}), T_a is the ambient gas temperature (K) and T_s is the surface temperature of the liquid particle K which can be predicted by the following relation [19]:

$$D(C_s - C_a) = k(T_a - T_s)/\lambda \quad (4)$$

where D is the diffusivity of H_2O in He (cm s^{-1}), and C_s and C_a are the water vapour concentration at the particle surface and at the ambient, respectively (gmol cm^{-3}). It was predicted for the first preheating zone kept at 60 °C that the gas was saturated with H_2O vapour and the droplet size decreased from 6.23 μm to 4.44 μm within 3×10^{-3} s while its temperature was 48 °C.

In the second preheating zone kept at 150 °C, the size of the liquid particle further decreased to 1.37 μm

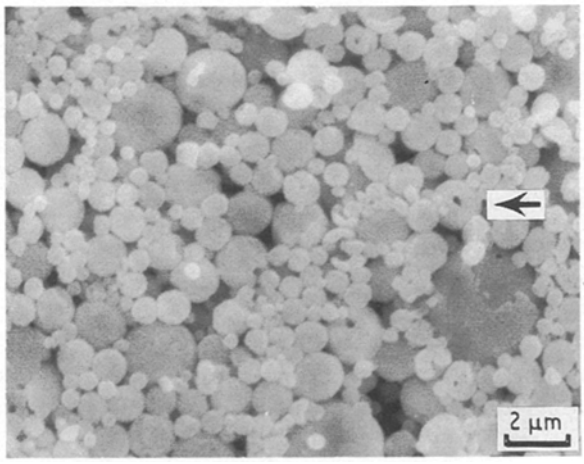

Figure 8 SEM micrograph of the $Pb(NO_3)_2$ particles synthesized at 150 °C and 3000 cc min^{-1} flow rate with a solution concentration of 3.24×10^{-2} mol l^{-1}.

within 1×10^{-3} s before $Pb(NO_3)_2$ started to precipitate. For the falling rate period, that is the rate that occurred during the drying of the solid particle, the following equation can be written [19]

$$\frac{dw'}{dt} = \frac{12k(T_a - T_s)}{\lambda d_c^2 \rho_s} \quad (5)$$

where dw'/dt is the drying rate ($g\,s^{-1}\,g^{-1}$ of solid), d_c is the critical particle size where the first precipitation of solid is observed, ρ_s is the density of the solid ($g\,cm^{-3}$). Equation 5 predicted that the particle was completely dried within 1×10^{-4} s.

$Pb(NO_3)_2$, in the liquid particle, precipitates after the liquid is supersaturated. Critical size of the precipitate can be calculated by the classical thermodynamic theory of nucleation [20]

$$d_c = \frac{12M\sigma}{3000\rho_s N_A kT \ln(W/W_{eq})} \quad (6)$$

where d_c is critical nucleus size (cm), M is molar weight ($g\,g^{-1}mol^{-1}$), N_A is Avagadro's number ($atoms\,g^{-1}mol^{-1}$), k is Boltzmann constant ($erg\,K^{-1}$), W and W_{eq} are the concentration of the solution and the solubility, respectively ($g/100\ g\ H_2O$). The metastable zone width, $\Delta W = W - W_{eq}$ and the surface energy $\sigma(erg\,K^{-1})$ were roughly estimated from Equation 3.9 and Fig. 3.8 given by Nyvlt [20]. The critical nucleus size, calculated for the solution supersaturated at 100 °C, was around 2.2 nm. The size of the microcrystals forming the $Pb(NO_3)_2$ particles given in Fig. 8 was 55.2 nm according to the Scherrer's equation.

As a result, it was shown that the gas residence time in the preheating sections (1.1–1.4 s) was sufficient enough for the complete drying of the liquid particles. It should also be noted that, according to the estimations, the gas was heated to the wall temperature within 10 cm (0.44–0.56 s) at each preheating section. Thus, the liquid particles shrunk and completely dried during the heating of the gas. Furthermore, the SEM micrographs, density and the surface analysis showed that the smooth drying of the liquid particles has been achieved at the exit of the second preheating zone resulting into fully dense, spherical and non-porous $Pb(NO_3)_2$ particles.

Investigations on the thermal decomposition of $Pb(NO_3)_2$ has shown that the decomposition proceeds through three or four reaction stages by the formation of lead oxide nitrate or nitrites [14, 15, 18, 21]. We have observed four reaction stages in DTA/TGA experiments (Fig. 3). The following four-stage dissociation mechanism has been proposed [14]:

$$Pb(NO_3)_2 \rightarrow 2PbO \cdot Pb(NO_3)_2 \rightarrow 3PbO \cdot Pb(NO_3)_2 \rightarrow 4PbO \cdot Pb(NO_3)_2 \rightarrow PbO \quad (7)$$

A 0.83 μm $Pb(NO_3)_2$ particle shrunk to a PbO particle as a result of pyrolysis reactions. Their sizes are related by the material balance as follows:

$$\frac{V_s}{V_o} = \frac{M_s \rho_o}{M_o \rho_s} \quad (8)$$

where V is the particle volume (cm^3), and subscripts s and o indicate the salt and oxide, respectively. The PbO particle size calculated by this equation was 0.57 μm and in very good agreement with the experimental value, 0.53 μm. Both of the $Pb(NO_3)_2$ and PbO particles were polycrystalline. The crystal size of the $Pb(NO_3)_2$ particles was 55.2 nm. Similarly, the crystal size of the PbO particles calculated by Equation 8 was 37.8 nm, which was again close to the experimental size, 28–35.5 nm.

Then, it was concluded that the conversion of a $Pb(NO_3)_2$ particle to a PbO particle occurred without any loss of the solid content. If this conversion occurred while the particle was solid, the particle would have burst into pieces because of the evolving gaseous reaction products from fully dense and non-porous particles. Therefore, it was expected that the $Pb(NO_3)_2$ decomposition occurred in the liquid phase allowing the smooth evolution of the gas formed within the particle by bubbling. Indeed, it was found that the mixtures of the product of the first decomposition stage, $2PbO \cdot Pb(NO_3)_2$ and $Pb(NO_3)_2$ melt at an eutectic point of 407 °C [14]. However, at the later stages of the dissociation, the eruptions from the particles, caused by gaseous products of nitrates or nitrites remaining in the particle in small quantities, left the particles with rough surfaces.

The following model was developed to determine the overall chemical reaction rate by assuming that the volume of the particle has linearly changed with the conversion and the overall decomposition has been a first-order reaction:

$$\ln \frac{V_t - V_\infty}{V_s - V_\infty} = k't \quad (9)$$

where subscripts ∞ and t denote the volume of the particle at infinite reaction time and at reaction time t, respectively. k' is the reaction rate constant (s^{-1}) and t is the reaction time (s). This model could reasonably explain the conversion data obtained from the experiments performed at 300–500 °C (see Fig. 9). The temperature dependency of the reaction rate constant was found to be

$$k' = 8.67 \times 10^6\, e^{-24200/RT} \quad (10)$$

where R is the ideal gas constant ($cal\,g^{-1}\,mol^{-1}\,K^{-1}$). The above reaction model predicted a 2% conversion

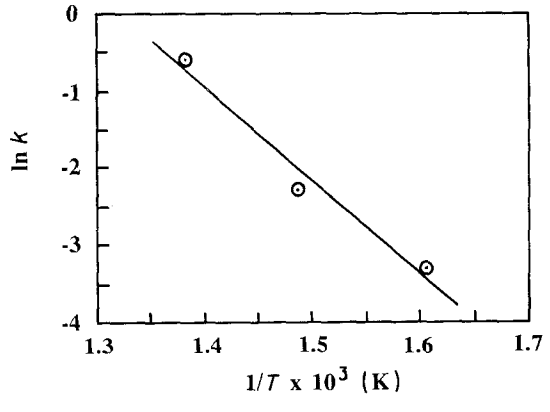

Figure 9 Effect of temperature on the decomposition rate of $Pb(NO_3)_2$.

at 300 °C and 96% at 500 °C whereas the experimental values were 1% and 97%. These results further confirmed that the model was reasonable. However, the previously reported activation energies have ranged between 37 and 57 kcal mol^{-1} [15]. The difference between the present and the reported values may therefore be due to the different techniques (TGA or the gasometric determination) used in the previous kinetic investigations which involved large sample amounts. It was predicted by Equations 9 and 10 that the reaction reached completion within 20 cm of the reactor length (L = 60 cm) at 700 °C.

Reactions reached almost completion at temperatures above 500 °C and the produced powders were mainly high purity tetragonal, red PbO. However, there was a continuing increase in the particle density with pyrolysis temperature (Table I). This result suggested that, after the completion of the reaction, initially, the powders contained closed porosity. At low pyrolysis temperatures, for example at 500 °C, the reactor length was just sufficient for completion of the reaction. Then, the sintering of the pores was not expected at these low temperatures. On the other hand, at high temperatures, for example at 700 °C, the reaction length was shorter than the reactor length, as discussed in the previous paragraph. Then, the closed pores could easily collapse resulting in a density increase as the particle residence time in the reactor was long and the temperature was high enough.

The high gas flow rate experiments yielded slightly purer and denser particles than that of the low gas flow rate experiments. This contradictory result was possibly due to the axial temperature profile forming in the pyrolysis section. The inlet of the pyrolysis section was around 655 °C when the centre temperature was 700 °C. It may be possible that the particles residing for a longer time in this section of the reaction tube at low flow rates can form a crust because of the decomposition reactions starting at the surface and proceeding to the centre of the particle due to the endothermic nature of the reaction. As a result of this, relatively less dense and impure PbO particles can be obtained. However, at high gas flow rates the particle may quickly reach the hotter sections of the reaction tube and, due to the high heat fluxes at these sections, the chemical reaction can simultaneously occur everywhere in the particle, preventing the formation of crust.

The particles had rough surfaces. These surfaces were possibly formed during the decomposition of the remaining precursor at later stages of the pyrolysis. Some experiments were attempted at 800 °C to smoothen the particle surfaces by melting. The melting point of PbO is 886 °C [11]. Unfortunately, these experiments were not successful, either the particles decomposed to other forms of lead oxide or the yield was very low. The low yield was attributed to evaporation of PbO. The reactor temperature towards the exit was 20–30 °C higher than the centre temperatures given in Table I. TGA data showed that, at these temperatures, PbO can appreciably evaporate which decreases the yield (Fig. 3). The eye observation of a white film on the reactor wall close to the exit also confirmed the evaporation of PbO from the particle and then the condensation on the wall.

However, the particles that synthesized at a lower salt concentration had smoother faceted surfaces than the particles discussed above. These particles were polycrystalline and had crystal sizes of 25 nm. Their faceted surfaces may be the manifestation of the inner crystal structure. In this case, the solution concentration was 4×10^{-3} mol l^{-1}. An eighth of the concentration, 3.24×10^{-2} mol l^{-1} was used to synthesize the 0.53 μm particles. Then, the expected size was found to be 0.27 μm from the relation between the concentration and the size. Indeed, the mean size of the particles shown in Fig. 7 was 0.27 μm suggesting that it is also possible to obtain dense particles at low concentrations.

In conclusion, based on the above predictions, the model schematically shown in Fig. 10 was proposed to explain the solid PbO particle formation from $Pb(NO_3)_2$ solution. Liquid particles form on the surface of the fountain by the rupture of the crests of the capillary waves generated by ultrasonic vibrations. These liquid particles grow by coagulation in the mist chamber. In the first preheating section, the liquid particles shrink by evaporation of water and in the second preheating section, they continue to shrink until $Pb(NO_3)_2$ starts to precipitate. Then, they are dried to non-porous, dense and spherical $Pb(NO_3)_2$ particles. These particles convert into the PbO particles in the pyrolysis section without any particles bursting due to the decomposition reactions occurring in the liquid phase. The small eruptions from the particles due to the unconverted precursor remaining inside the particle generate rough particle surfaces.

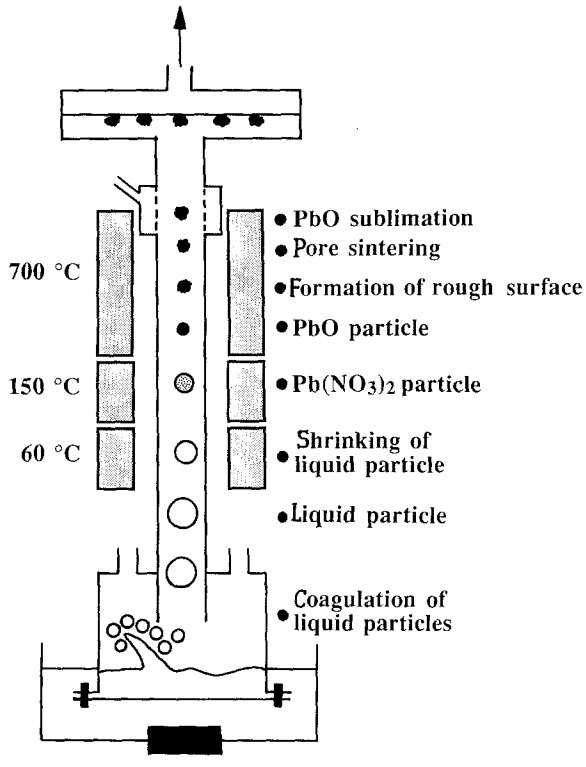

Figure 10 The schematic representation of the PbO particle formation from the $Pb(NO_3)_2$ solution.

Finally, the pores collapse at high temperatures, forming non-porous and dense PbO particles. If the pyrolysis temperatures are high enough, the particle yields will decrease by sublimation of PbO from the particle.

5. Conclusions

High purity, fully dense, submicrometer (< 0.53 μm) and non-agglomerated PbO particles were continuously produced by spray pyrolysis of $Pb(NO_3)_2$ solution in a tubular-flow reactor using an ultrasonic mist generator. $Pb(NO_3)_2$ particles could be completely converted to crystalline, mainly tetragonal PbO at temperatures above 500 °C. Preliminary experiments indicated that the particle size can successfully be decreased by decreasing the concentration of the salt solution. The high particle yields ($> 90\%$) obtained at high flow rates indicated the high efficiency of the technique.

Preheating of the mist before the pyrolysis stage by two heaters maintained at different temperatures was found to be necessary to obtain fully densified particles. It was experimentally shown that completely dried, dense and non-porous $Pb(NO_3)_2$ particles are produced at the end of the preheating section. It is expected that these non-porous particles will be broken into small pieces due to the gases produced inside the particle during decomposition reactions. However, it was experimentally observed that the decomposition and the shrinking of a $Pb(NO_3)_2$ particle to a PbO particle occurred without any loss in its solid content, indicating that the expected particle explosion did not occur. Therefore, it was thought that the decomposition occurred through the liquid phase allowing the evolution of the gaseous reaction products by bubbling.

The experimentally obtained particle size, 53 μm was bigger than that predicted by theory, 0.27 μm. The coagulation of the spray particles in the vicinity of the fountain generated by high frequency ultrasonic vibrations was thought to be responsible for this particle growth. It was predicted that the spray was quickly dried to the salt particles. The reaction model, developed by assuming first order reaction rate and linear shrinking of the particle volume, could explain the decomposition of the salt particles.

It was found by i.r. analysis that the particles contained small amounts of unconverted material (< 2–3%) at low gas flow rates although the pyrolysis temperature was as high as 700 °C, because of the trapped material inside the particle during the pyrolysis processes. Increasing the gas flow rate increased both the density and purity of the particle. This result contradicting usual expectations was attributed to the axial temperature profile formed in the pyrolysis heater.

Acknowledgement

The authors wish to acknowledge gratefully the Directorate of Chemical and Atmospheric Sciences of the Air Force Office of Scientific Research for providing financial support for this work.

References

1. B. DUBOIS, D. RUFFIER and P. ODIER, *J. Amer. Ceram.* **72** (1989) 713.
2. T. J. GARDNER, D. W. SPROSON and G. L. MESSING, *Mater. Res. Soc. Symp. Proc.* **32** (1984) 227.
3. H. ISHIZAWA, O. SAKURAI, N. MIZUTANI and M. KATO, *Amer. Ceram. Soc. Bull.* **65** (1986) 1399.
4. Y. KANNO and T. SUZUKI, *J. Mater. Sci.* **23** (1988) 3067.
5. T. Q. LIU and O. SAKURAI, *ibid.* **21** (1986) 3698.
6. K. SEITZ, E. IVERS-TIFEE, H. THOMANN and A. WEISS, in "High technology ceramics", edited by P. Vincenzini (Elsevier, Amsterdam, 1987) p. 1753.
7. S. C. ZHANG, G. L. MESSING and M. BORDEN, *J. Amer. Ceram. Soc.* **73** (1990) 61.
8. O. G. RAABE, in "Fine particles: aerosol generation, measurement, sampling and analysis", edited by Liu (Academic Press, New York, 1976) 60.
9. D. H. CHARLESWORTH and W. R. MARSHALL, *AIChE J.* **6** (1960) 9.
10. F. KIRKBIR and H. KOMIYAMA, *Can. J. Chem. Engng* **65** (1987) 759.
11. J. A. DEAN, Ed., in "Lange's handbook of chemistry" (McGraw-Hill, New York, 1985) pp. 4–66, 4–68.
12. KIRK and OTHMER, in "Encyclopedia of chemical technology", Vol. 14 (John Wiley, New York, 1985) p. 164.
13. Standard Infrared Grating Spectra (Sadtler Res. Lab., Philadelphia, 1974) 33682K.
14. E. V. MARGULIS, M. M. SHOKAREV, L. A. SAVCHENKO, L. I. BEISEKEEVA and F. I. VERSHININA, *Russ. J. Inorg. Chem.*, **17** (1972) 21.
15. K. C. PATIL, R. K. GOSAVI and C. N. R. RAO, *Inorg. Chim. Acta.* **1** (1967) 155.
16. R. J. LANG, *J. Acoust. Soc. Amer.* **34** (1962) 6.
17. S. K. FRIEDLANDER, in "Smoke, dust, haze" (John Wiley, New York, 1977) p. 181.
18. F. VRATNY and F. GUGLIOTTA, *J. Inorg. Nucl. Chem.* **25** (1963) 1129.
19. K. MASTERS, in "Spray drying handbook", 4th ed. (George Godwin, London, 1985) p. 301.
20. J. NYVLT, in "The kinetics of industrial crystallization" (Elsevier, Amsterdam, 1985) p. 43.
21. K. H. STERN, *J. Phys. Chem. Ref. Data* **1** (1972) 758.

Received 29 August 1990
and accepted 31 January 1991